Accurate SNR Estimation in C+L-band 10-THz Hybrid Raman-EDFA Amplified Transmission Using Two-Stage Power Profile Calculation Accounting for Pump Depletion

Kosuke Kimura, Shimpei Shimizu, Takayuki Kobayashi, Masanori Nakamura, and Yutaka Miyamoto
NTT Network Innovation Laboratories, NTT corporation,1-1 Hikarinooka, Yokosuka, Kanagawa, Japan
E-mail address: kousuke.kimura@ntt.com

Abstract: We propose an accurate power profile calculation method for GN-model-based SNR estimation and demonstrate an average SNR estimation error of 0.22 dB in C+L-band 101-ch WDM 96-Gbaud PCS-36QAM signal 1120-km hybrid Raman-EDFA amplified transmission.

1. Introduction

Ever-increasing traffic has led to the development of ultra-wideband (UWB) wavelength division multiplexing (WDM) transmission technologies [1–5], increasing the need for complex optimization (e.g., the launch power of each channel) with frequency-dependent parameters to maximize system throughput. The optimization requires system performance to be predicted with high computational efficiency, which can be done by using nonlinear interference (NLI) estimation based on the Gaussian noise (GN) model [6]. NLI models have been proposed for UWB WDM systems, enabling efficient and accurate evaluation of system performance [7–10]. For hybrid distributed Raman-EDFA amplified transmission, analytical and experimental investigation of GN-model-based SNR estimation has been conducted in [11]. One of the key steps for accurate SNR estimation is calculating the signal power profile along the fiber's longitudinal and frequency directions by solving coupled Raman equations, which affects the prediction of ASE and NLI-induced penalties.

In this paper, we propose an accurate signal power profile calculation method taking into account the depletion of backward Raman pumps. This method solves coupled Raman equations iteratively and consists of two stages to speed up the calculation. We verify that the proposed method enables accurate estimation of the effective noise figure (NF) of distributed Raman amplification as well as signal power profiles. Using the proposed method, we demonstrate sufficiently accurate SNR estimation with an average estimation error of 0.22 dB in a C+L band 101-ch WDM 96-Gbaud probabilistically constellation-shaped (PCS)-36QAM signal transmission experiment over 1120-km G.652.D single-mode fiber (SMF) with hybrid backward distributed Raman-EDFA amplification.

2. Power profile calculation in systems with backward distributed Raman amplification

This chapter outlines our proposed signal power profile calculation method. The method takes into account the pump depletion (PD) of backward Raman pumps, which is the depletion of pump power due to power transfer from pumps to signals. Pump depletion increases with signal launch power, which can result in prediction errors for ASE and NLI-induced penalties. Although accounting for the PD increases computational complexity, this makes it possible to avoid overestimating Raman gain. In the proposed method, coupled Raman equations are solved iteratively in the forward and backward directions. The input to the calculation is the input spectra of a WDM signal $\boldsymbol{P_{sig}}(0) = [P_1(0), P_2(0), \cdots, P_k(0)]^T$ and backward Raman pumps $\boldsymbol{P_{bp}}(L) = [P_{k+1}(L), P_{k+2}(L), \cdots, P_N(L)]^T$ into an optical fiber transmission line, where $i = 1, 2, \cdots, N$ is the frequency index, $P_i(z)$ is optical power, z is a position along the fiber span of length L, and frequency f_i is in the ascending order. We assume that the fiber loss spectrum and Raman gain coefficient C_R, which are required for solving coupled Raman equations, are known. The calculation consists of two stages shown in Fig. 1. The first stage is a coarse calculation assuming PD is frequency-independent to obtain approximately accurate profiles quickly. The second stage is a fine calculation that accounts for frequency-dependent PD to obtain accurate power profiles. Combining the two stages can speed up power profile calculation.

The first stage minimizes a cost function f_{cost} with respect to a frequency-independent update coefficient X subject to $\exp\left(-max(C_R)\sum \boldsymbol{P_{sig}}(0)L\right) \leq X \leq 1$. The left side is a quantity that overestimates PD and is derived

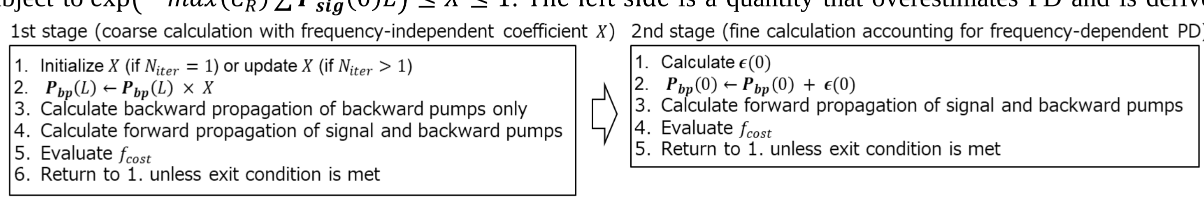

Fig. 1 Proposed method for power profile calculation accounting for pump depletion.

from an analogy with closed-form on-off Raman gain ignoring PD. f_{cost} is defined to quantify the error between the re-calculated and original input pump spectra at $z = L$ as in [7]. The original $\boldsymbol{P_{bp}}(L)$ is the spectrum inputted first. f_{cost} decreases as PD is accurately accounted for in the power profile calculation. First, X is initialized or updated (step 1: s1) using optimization algorithms such as the golden-section search. Using $\boldsymbol{P_{bp}}(L)$ multiplied by X (s2), the backward propagation of only backward pumps is calculated to determine $\boldsymbol{P_{bp}}(0)$ (s3). After combining $\boldsymbol{P_{bp}}(0)$ and $\boldsymbol{P_{sig}}(0)$, the forward propagation of the signal and pumps is calculated to obtain $\boldsymbol{P_{bp}}(L)$, which is the re-calculated pump spectrum (s4). f_{cost} is evaluated on the basis of the obtained $\boldsymbol{P_{bp}}(L)$ (s5). These procedures are iterated until the exit condition (e.g., $f_{cost} \leq$ threshold) is satisfied. The last $\boldsymbol{P_{sig}}(z)$ and $\boldsymbol{P_{bp}}(z)$ are passed onto the second stage.

In the second stage, error vector $\boldsymbol{\varepsilon}(0) = [\varepsilon_{k+1}(0), \varepsilon_{k+2}(0), \cdots, \ \varepsilon_N(0)]$ for updating $\boldsymbol{P_{bp}}(0)$ while accounting for the frequency dependence of PD is calculated based on $\boldsymbol{P_{sig}}(z)$ and $\boldsymbol{P_{bp}}(z)$ (s1). The equation for calculating $\boldsymbol{\varepsilon}(0)$ is obtained by submitting $\boldsymbol{P_{sig}}(z) + \ w \times \boldsymbol{\varepsilon}(z)$ to coupled Raman equations, where w is a weight for updating, while regarding the error vector as perturbation as in [12]. The equation is summarized as $\boldsymbol{\varepsilon}(0) = \ (\prod_{z=0}^{L-dz} M(z))^{-1}\boldsymbol{\varepsilon}(L)$, where $M(z)$ is an $(N-k) \times (N-k)$ matrix, and $\boldsymbol{\varepsilon}(L)$ is the difference between the calculated and original $\boldsymbol{P_{bp}}(L)$. This is a linear equation for updating $\boldsymbol{P_{bp}}(0)$ multi-dimensionally at once, enabling faster convergence of power profiles than the nonlinear least-squares method by a factor of approximately the number of dimensions of $\boldsymbol{P_{bp}}(\boldsymbol{z})$. After calculating $\boldsymbol{\varepsilon}(0)$, $\boldsymbol{P_{bp}}(0)$ is updated (s2). The updated $\boldsymbol{P_{bp}}(0)$ is used to calculate the forward propagation of signal and backward pumps (s3), giving $\boldsymbol{P_{bp}}(L)$. The remainder of the procedure is the same as that of the first stage.

3. Experimental validation

Figure 2 (a) shows an experimental setup of C+L-band 10-THz WDM hybrid backward distributed Raman-EDFA amplified transmission. A 100-GHz-spaced 101-ch (42-ch in the C-band and 59-ch in the L-band) WDM signal was emulated by amplified spontaneous emission (ASE). The C-band signal ranged from 1528.00 to 1561.42 nm, and the L-band signal ranged from 1570.01 to 1620.06 nm. The total signal bandwidth was 10.1-THz. The measurement channel was a Nyquist-pulse-shaped 96-Gbaud polarization-multiplexed PCS-36QAM signal. The re-circulating transmission line consisted of gain blocks 1 and 2, an 80-km G.652.D SMF, Raman pumps, and optical components for re-circulation. Raman pumps at 1430, 1450, 1480, and 1505 nm were used. Each gain block was a lumped repeater consisting of C- and L-band EDFAs. The total input power of the Raman pumps into the G.652.D SMF was 27.8 dBm. The WDM signal was equalized by gain equalizers (GEQs) in gain block 2. After the 1120-km transmission, the measurement channel was demodulated by offline digital signal processing based on a complex 8×2 MIMO equalizer [13], and the SNR was evaluated from the variance of the recovered symbols. Figure 2 (b) and (c) show the measured gains and NFs of gain blocks 1 and 2. These were used to calculate the generalized optical signal to noise ratio (GOSNR) of each WDM channel, which includes the back-to-back characteristic and accumulated ASE and NLI. NLI was estimated by combining power profile calculation and a GN method [14]. The GOSNR was converted to an SNR as in Fig. 2 (d), which shows the relationship between the OSNR (noise bandwidth = 12.5 GHz) and the SNR measured at 1544 nm in the back-to-back configuration. The estimated SNRs were compared with the measured SNRs.

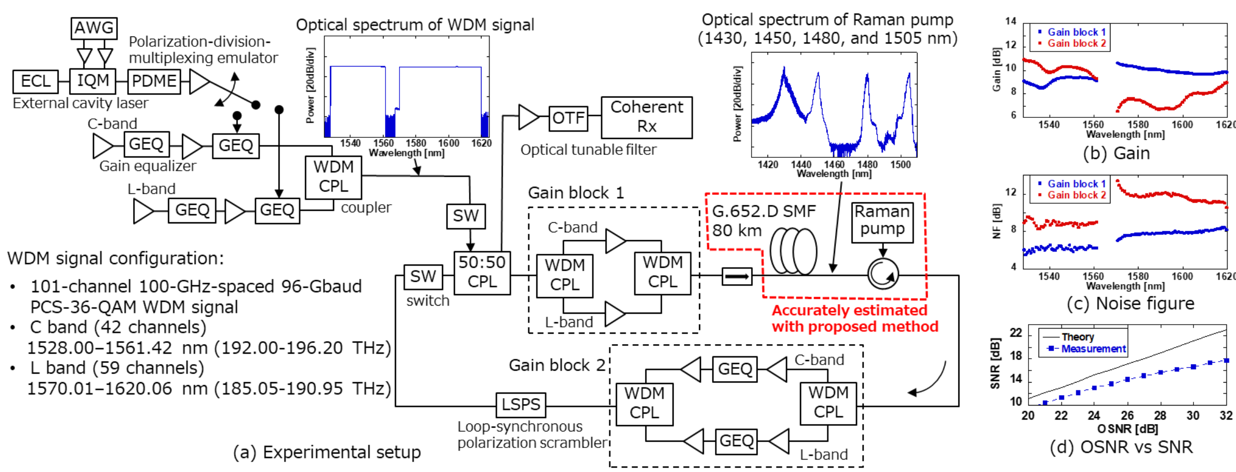

Fig. 2 (a) Experimental setup, (b) gain and (c) noise figure (NF) of gain block 1 and 2, and (d) OSNR (noise bandwidth = 12.5 GHz) vs. SNR measured in back-to-back configuration.

4. Results

Figure 3 (a) shows the on-off Raman gain averaged over frequency for different WDM signal launch powers, and Fig.

3 (b) and (c) show the on-off gain spectra at launch powers of 11 dBm (small PD) and 23 dBm (large PD), respectively. The black plots are the measured results of the experiment. The blue and red plots are the estimated results without PD and with PD, respectively. The SRS between pumps was taken into account even in the estimation without PD. Although the gain estimated without PD deviated from the measured gain for high launch powers, the estimated gain with PD agreed well with the measured gain. The estimation without PD increases estimation errors especially in the L-band (see Fig. 3 (c)) because the on-off gain in longer wavelengths increases due to inter-pump SRS. These results demonstrate that the proposed method enables accurate power profile calculation by taking into account the PD. Similarly, Fig. 4 (a) shows the effective NFs of the Raman amplification averaged over frequency for different launch powers, and Fig. 4 (b) and (c) show effective NF spectra at launch powers of 11 dBm and 23 dBm, respectively. The measured effective NFs were evaluated at five wavelengths in each of the C- and L-bands. The estimated effective NFs are quantified by calculating accumulated ASE involved with distributed Raman amplification based on power profiles as in [15, 16]. These results demonstrate that the proposed power profile calculation also enables accurate effective NF calculation. Finally, Fig. 5 shows the SNRs of 101 WDM channels after the 1120-km transmission at a launch power of 20 dBm. The ratio of the back-to-back penalty, ASE from gain blocks 1 and 2, ASE from Raman amplification and NLI was approximately 3.3:5.4:2.1:1.0 in this condition. The average SNR estimation error was improved from 0.40 dB to 0.22 dB by using the proposed power profile calculation method.

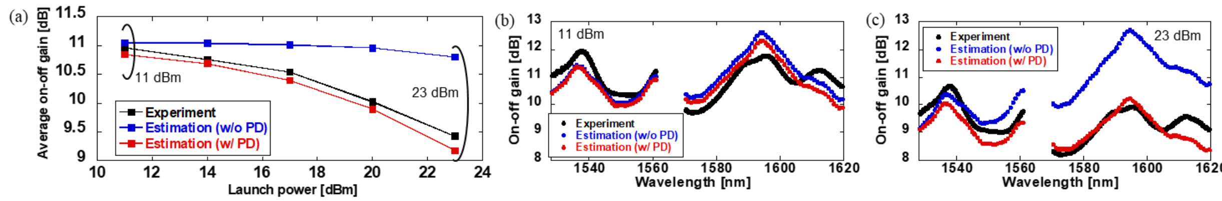

Fig. 3 (a) On-off Raman gain averaged over frequency vs. WDM signal launch powers, on-off Raman gain spectra at launch powers of (b) 11 dBm and (c) 23 dBm.

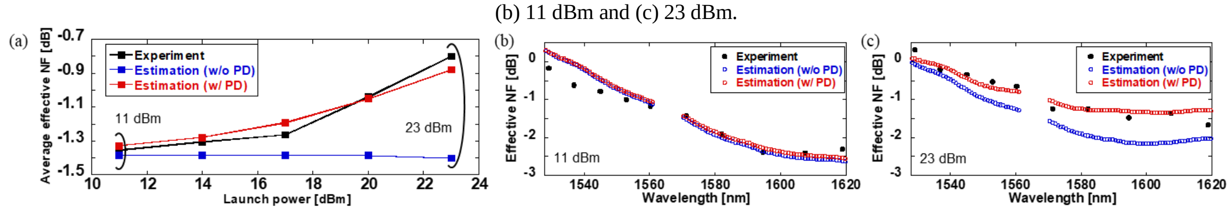

Fig. 4 (a) Effective noise figure (NF) of Raman amplification averaged over frequency vs. WDM signal launch power, effective NF spectra at launch powers of (b) 11 dBm and (c) 23 dBm.

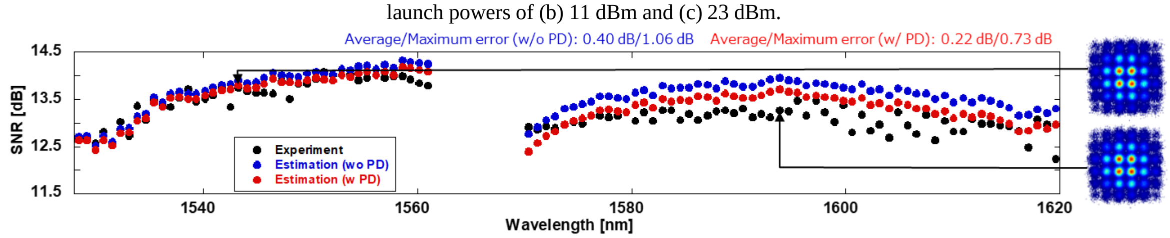

Fig. 5 SNRs of 101 WDM channels after 1120-km transmission at a launch power of 20 dBm.

5. Conclusion

We proposed a two-stage iterative calculation method for efficient and accurate calculation of power profiles while accounting for pump depletion. The proposed method enables faster convergence of power profiles than the nonlinear least-squares method by a factor of approximately the number of dimensions of $\boldsymbol{P_{bp}(z)}$. We demonstrated an average SNR estimation error of 0.22 dB in C+L-band 101-ch WDM 96-Gbaud PCS-36QAM signal transmission over 1120-km G.652.D SMF with hybrid backward distributed Raman-EDFA amplification using the power profile calculation.

References

[1] F. Hamaoka, in Proc. OECC2022, PDP-A-3.
[2] A. Ghazisaeidi et al., J. Lightw. Technol., 40, 21, 7014-7019, 2022.
[3] T. Kobayashi et al., in Proc. OFC2023, Th4B.6.
[4] D. Soma et al., in Proc. ECOC2023, Th.C.2.2.
[5] B. Puttnam et al., in Proc. ECOC2023, Th.C.2.4.
[6] P. Poggiolini, J. Lightw. Technol., 30, 24, 3857-3879, 2012.
[7] M. Ranjbar Zefreh et al., arXiv:2006.03088, 2020.
[8] P. Poggiolini et al., in Proc. ECOC2022, Tu1D.1.
[9] H. Buglia et al., J. Lightw. Technol., 1-13, 2023.
[10] H. Buglia et al., in Proc. ECOC2023, P4.
[11] L. Galdino et al., J. Lightw. Technol., 37, 21, 2019.
[12] K. Fujimura et al., in Proc. OAA2003, MC3, 2003.
[13] T. Kobayashi et al., in Proc. OFC2019, Th4B.2, 2019.
[14] M. Ranjbar Zefreh et al., ArXiv200912687, 2020.
[15] S. R. Chinn, Electron. Lett., 33, 7, 607-608, 1997.
[16] B. Mukherjee et al., Springer Handbook of Optical Networks (Springer, 2020), Chap 3.